




A Hybrid Asynchronous Brain-Computer Interface Combining SSVEP and EOG Signals

Yajun Zhou , Shenghong He , Qiyun Huang, and Yuanqing Li , *Fellow, IEEE*

Abstract—Objective: A challenging task for an electroencephalography (EEG)-based asynchronous brain-computer interface (BCI) is to effectively distinguish between the idle state and the control state while maintaining a short response time and a high accuracy when commands are issued in the control state. This study proposes a novel hybrid asynchronous BCI system based on a combination of steady-state visual evoked potentials (SSVEPs) in the EEG signal and blink-related electrooculography (EOG) signals. **Methods:** Twelve buttons corresponding to 12 characters are included in the graphical user interface (GUI). These buttons flicker at different fixed frequencies and phases to evoke SSVEPs and are simultaneously highlighted by changing their sizes. The user can select a character by focusing on its frequency-phase stimulus and simultaneously blinking his/her eyes in accordance with its highlighting as his/her EEG and EOG signals are recorded. A multifrequency band-based canonical correlation analysis (CCA) method is applied to the EEG data to detect the evoked SSVEPs, whereas the EOG data are analyzed to identify the user's blinks. Finally, the target character is identified based on the SSVEP and blink detection results. **Results:** Ten healthy subjects participated in our experiments and achieved an average information transfer rate (ITR) of 105.52 bits/min, an average accuracy of 95.42%, an average response time of 1.34 s and an average false-positive rate (FPR) of 0.8%. **Conclusion:** The proposed BCI generates multiple commands with a high ITR and low FPR. **Significance:** The hybrid asynchronous BCI has great potential for practical applications in communication and control.

Index Terms—Asynchronous brain-computer interface (BCI), electroencephalography (EEG), steady-state visual evoked potential (SSVEP), electrooculography (EOG), eye blink.

I. INTRODUCTION

IN RECENT years, research on brain-computer interfaces (BCIs), which enable the translation of neural activities into control commands for external devices without the participation of peripheral nerves and muscles [1], has witnessed tremendous development. Electroencephalography (EEG) is commonly used in noninvasive BCI systems due to its ease of data acquisition and high temporal resolution [2], [3]. The typical EEG brain activity patterns used in BCIs include motor imagery-related synchronization/desynchronization (ERD/ERS) [4], [5], P300 potentials [6], [7] and steady-state visual evoked potentials (SSVEPs) [8], [9]. An EEG-based BCI can be synchronous or asynchronous. A BCI is synchronous if the time at which a command is issued is controlled by the computer [10], [11], whereas in an asynchronous BCI system, users choose to issue a command at their discretion or to remain in the idle state for a long period [10], [12].

An ideal asynchronous BCI must effectively distinguish between the idle and control states, which requires a low false-positive rate (FPR) in the idle state and a low false-negative rate (FNR) in the control state. Furthermore, a short response time and a high accuracy must be maintained when control commands are issued in the control state. A strict threshold criterion is generally used to decrease the FPR in the idle state. However, imposing this criterion will increase the response time when a control command is issued and the FNR in the control state. In contrast, a lax threshold condition potentially reduces the response time; however, it will also lead to a high FPR in the idle state, and thus, many control commands might be incorrectly generated in the idle state. Therefore, a challenging task is to establish an asynchronous BCI system with high performance in effectively distinguishing between idle and control states.

Recently, various synchronous/asynchronous BCIs have been proposed based on different brain signals. Among these systems, SSVEP-based BCI systems have the advantage of a relatively high information transfer rate (ITR). When a subject focuses on a visual stimulus that is steadily flickering at a certain frequency, a resonance will be elicited in the visual cortex at that specific frequency and its harmonics, i.e., an SSVEP [13], [14]. Based on this phenomenon, a flickering target can be selected based on the

Manuscript received November 1, 2019; revised January 16, 2020; accepted February 1, 2020. Date of publication February 11, 2020; date of current version September 18, 2020. This work was supported in part by the National Natural Science Foundation of China under Grant 61633010, in part by the National Key Research and Development Program of China under Grant 2017YFB1002505, in part by the Guangdong Natural Science Foundation under Grant 2014A030312005, and in part by the Key R&D Program of Guangdong Province, China under Grant 2018B030339001. (Corresponding author: Yuanqing Li.)

Yajun Zhou and Qiyun Huang are with the School of Automation Science and Engineering, South China University of Technology, and the Guangzhou Key Laboratory of Brain Computer Interface and Applications (no. 15180006).

Shenghong He is with the MRC Brain Network Dynamics Unit and Nuffield Department of Clinical Neurosciences, University of Oxford.

Yuanqing Li is with the School of Automation Science and Engineering, South China University of Technology, and the Guangzhou Key Laboratory of Brain Computer Interface and Applications (no. 15180006), Guangzhou 510640, China (e-mail: auyqli@scut.edu.cn).

This article has supplementary downloadable material available at <http://ieeexplore.ieee.org>, provided by the authors.

Digital Object Identifier 10.1109/TBME.2020.2972747

detection of the evoked SSVEP. In recent years, the canonical correlation analysis (CCA)-based algorithm has been proven to be an efficient tool for recognizing the target frequency [15]. For example, Chen *et al.* developed a synchronous system that achieved a relatively high ITR of 5.32 bits per second in a 40-character spelling experiment [16]. Various threshold criteria have been proposed, such as a feature model based on kernel CCA coefficients [11], an approximate fractal entropy [17], and a maximum evoked response spatial filter [18], to improve the performance of SSVEP-based asynchronous BCIs in distinguishing between the idle and control states. Furthermore, several specific paradigms have been developed, such as one involving a flickering target key and several flickering pseudokeys [19]. According to the existing results for SSVEP-based BCI systems, the performance in the asynchronous mode is much less satisfactory than the performance in the synchronous mode.

Motor imagery (MI) [20], [21], which enables a self-paced control approach for subjects, has also been used to develop asynchronous BCIs, despite the limited number of commands available (usually only two). Liu *et al.* [22] proposed an adaptive threshold method based on a set stop time for a BCI using left- and right-hand MI. The reported average accuracy and response time were 83.4% and 2.77 s, respectively. A receiver operating characteristic (ROC) curve is commonly used to define the thresholds and evaluate the performance of asynchronous MI systems [23]. Other researchers have developed asynchronous BCIs based on P300 potentials evoked in the “odd-ball” paradigm. For example, Martínez-Cagigal *et al.* [24] reported a P300-based asynchronous web browser with a preset threshold and a stepwise linear discriminant analysis model that enabled several patients with sclerosis to communicate with an average FPR of 4.61%. The authors of another study [25] developed their P300-based asynchronous BCI by calculating the likelihood of the control state based on a support vector machine (SVM) regression model and reported an average ITR and FPR of 20 bits/min and 1 event per minute, respectively.

Unlike EEG signals, electrooculography (EOG) signals are induced by eye movements (blinking, fixating, and looking in different directions). Because of their strong amplitudes, EOG signals are usually easier to detect and more stable across different subjects than EEG signals [26]. Several asynchronous systems based on eye movement identification have been used in various applications, such as text spelling [27] and robot control [28].

A hybrid BCI is generally composed of one BCI and another system (which might be another BCI) and can achieve specific goals better than a conventional BCI [29]. For instance, several hybrid BCIs were presented for MI training with SSVEP feedback [30], preventing unexpected spelling error using SSVEPs and eye tracking [31], or improving ITR using EEG and near-infrared spectroscopy (NIRS) [32], [33]. An asynchronous BCI can also be implemented based on a hybrid approach integrating multiple brain patterns, such as SSVEP combined with MI [34], SSVEP combined with P300 potential [35], or P300 potential combined with EOG data [36].

However, these existing systems have not been able to achieve relatively rapid and accurate output decisions in the control state

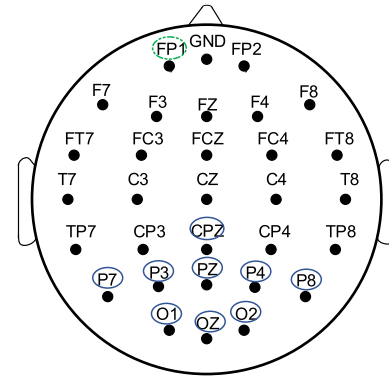


Fig. 1. Channel configuration for EEG (blue solid circles) and EOG (green dotted circle).

and a low FPR over a long period in the idle state (usually, the FPR is greater than 3%).

In this paper, we propose a new method of improving the performance of an asynchronous BCI by combining SSVEP and EOG signals. Twelve buttons corresponding to 12 characters are included in the graphical user interface (GUI) and flicker at different frequencies and phases to evoke SSVEPs. Simultaneously, these buttons are highlighted by suddenly reducing their sizes to provide cues (timestamps) for the user to blink his/her eyes. The user must perform two tasks to issue a command: gazing at the frequency-phase stimulus of the target character and blinking his/her eyes in synchrony with its highlights. A CCA method based on a subband combination is used to detect the SSVEPs, and an EOG waveform analysis method is applied to identify blinks. The combination of SSVEP and blink detection is used not only for control/idle state differentiation but also for the recognition of the target character in the control state. Ten healthy subjects participated in our experiments. Based on the results of the experiment, the proposed SSVEP- and EOG-based asynchronous BCI system displays satisfactory performance, with an average ITR of 105.52 bits/min, an average accuracy of 95.42%, an average response time of 1.34 s when a command is issued, and an average FPR of 0.8%.

The remainder of this paper is organized as described below. Section II describes the methods, including the data acquisition, GUI, and signal processing algorithms for SSVEP and blink detection. Section III presents the experimental results. Section IV provides further discussion, and Section V describes the conclusions of the paper.

II. MATERIALS AND METHODS

A. EEG and EOG Data Recording

EEG and EOG data were recorded using a Synamps2 system (Neuroscan, Inc.) with a sampling rate of 250 Hz. The electrodes placed on the forehead (GND) and right mastoid (A2) were used as the ground and reference electrodes, respectively. Nine channels in the occipital region, including CPz, P7, P3, Pz, P4, P8, O1, Oz and O2 based on the standard positions in the 10–20 system, were chosen for acquiring EEG data [37], and one channel on the forehead (Fp1) was used to record EOG data (Fig. 1). The impedances of the electrodes were maintained at

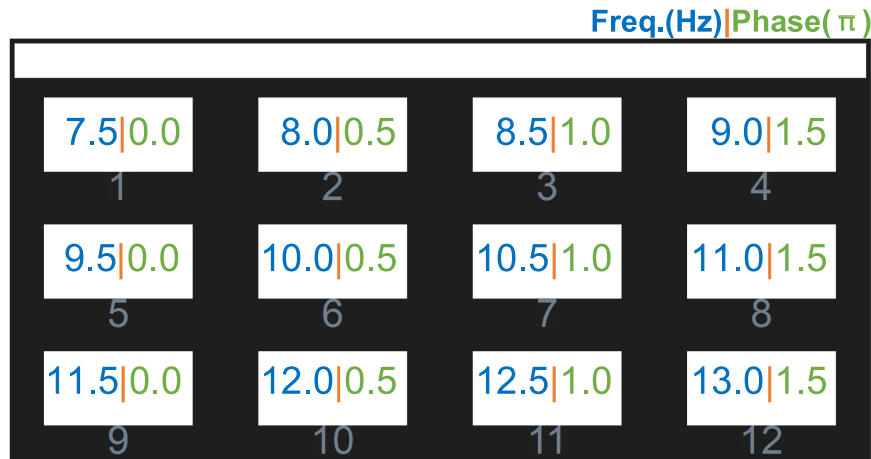


Fig. 2. Layout of the buttons displayed on the GUI for periodic sinusoidal visual stimulation, with their frequencies and phases indicated. The frequencies range from 7.5 Hz to 13.0 Hz in intervals of 0.5 Hz. The phase difference between two neighboring buttons is 0.5π .

levels less than 10 k Ω . The EEG signals were filtered using an 11th-order Butterworth bandpass filter with a frequency band of 6–70 Hz before further analysis, whereas the EOG signals were filtered to a range of 1–10 Hz with a 2nd-order Butterworth bandpass filter.

During the experiments, the subjects were asked to sit in front of a 23.6-inch liquid-crystal screen with a resolution of 1,920 \times 1,080 pixels and a refresh rate of 60 Hz. In the online experiment, the EEG and EOG data were both recorded and analyzed using the online data analysis program in real time, which was developed in MATLAB.

B. GUI and Stimulation Paradigm

As illustrated in Fig. 2, this study employs a periodic sinusoidal visual stimulation paradigm that incorporates both frequency and phase information to evoke SSVEPs, similar to the joint frequency-phase modulation (JFPM) paradigm proposed by Chen *et al.* [16]. The sinusoidal visual stimulation efficiently mitigates the problem of frequency limitation due to the screen refresh rate [38]. Furthermore, the phase information has been proven to be a good supplement to enhance the differentiation between SSVEPs at adjacent frequencies. Specifically, 12 buttons that are evenly distributed on the interface are flickering at different frequencies (ranging from 7.5 Hz to 13.0 Hz in intervals of 0.5 Hz) and phases (0, 0.5π , 1π , or 1.5π). Then, the periodic sinusoidal signals used to construct the frequency stimuli are modulated as follows:

$$x_k(t) = \sin\{2\pi[f_0 + (k-1)\Delta f]t + [\phi_0 + (k-1)\Delta\phi]\}, k = 1, \dots, K \quad (1)$$

where ϕ_0 (0, in this study) represents the initial phase of the target at f_0 (7.5 Hz); k is the index of the target, and K is the total number of targets; Δf (0.5 Hz) and $\Delta\phi$ (0.5π) are the frequency interval and phase interval, respectively.

Simultaneously, these buttons are also highlighted for the user to blink his/her eyes. A detailed description of the presentation of highlights is provided below. First, the 12 buttons were randomly

divided into six groups of two buttons each, with the constraint that the difference between the highlight index corresponding to the two buttons in each group is no less than three, e.g., $\{[9, 4], [1, 7], [10, 3], [6, 12], [2, 8], \text{ and } [5, 11]\}$. Using this approach, we ensured that the two buttons in each group were not spatially adjacent to each other. Next, each of the six groups of buttons were highlighted sequentially. Specifically, the two buttons in the chosen group were simultaneously highlighted by suddenly changing the size of each button from its original size to approximate three-quarters of the size. Each highlight was presented for 100 ms. Note that the highlighting form of changing these buttons' sizes rather than the flashing method used in other EOG or P300 studies [7], [27] was applied to avoid affecting the frequency-phase stimuli for SSVEP evocation. Additionally, this period during which each group of buttons are highlighted once with an interval of 500 ms after the onset of final highlight is defined as a round. The duration of a round of highlights may vary across subjects and was determined through a calibration process (in this study, the durations ranged from 1 s to 1.4 s for different subjects). The time interval between two adjacent rounds was 0.5 s, when a character was detected by the algorithm and presented, or 0 s, when no character was detected. Additionally, the first highlight was presented at 200 ms into the round, and the time interval between two adjacent highlights was determined in accordance with the length of the round. For example, the interval was 100 ms for a round length of 1.2 s. In this case, the highlight of the last button group occurred at 0.7 s ($=200 \text{ ms} + 5 \times 100 \text{ ms}$), and the EOG data corresponding to the last button group were collected in the remaining 500 ms (from the onset of the sixth highlight to the end of this round).

Fig. 3 illustrates the paradigm for the procedure of the stimulation, processing of EEG and EOG signals, and the final decision making process during one representative trial of the online experiments. Here, one trial is defined as the process from the stimulation onset to the time that a decision result is generated. Specifically, each trial consists of one or two stimulation rounds and a trial shifting time of 0.5 s (i.e., the blank from the end of stimulation in a trial to the beginning of the next trial). A detailed

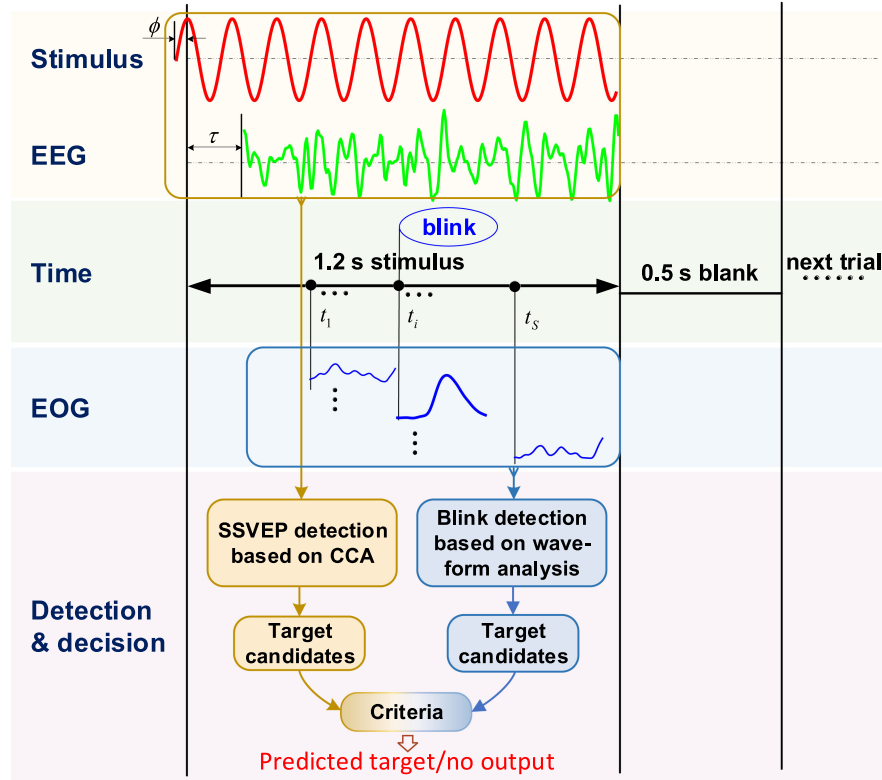


Fig. 3. Procedure used for spelling a target (e.g., the character “2” with 8.0 Hz, 0.5π) based on the proposed asynchronous system. The JFPM paradigm with different initial phases (ϕ) for different frequencies is used to evoke SSVEPs. An EEG epoch of 1.2 s with a time delay (τ) is collected for SSVEP detection. Meanwhile, EOG segments from a single round after the highlight onset (at the time of t_k , $k \in [1, 2, \dots, S]$, S is six in this study) are collected for blink detection. Finally, based on the results of SSVEP and blink detections, a decision is made. Specifically, if all criteria are satisfied, a predicted target is obtained; otherwise, no output is generated.

description of signal processing and the decision process is provided below. (denoted by \mathbf{Y}_f) is presented below:

C. EEG Signal Processing

In offline and online experiments, data epochs of SSVEPs were extracted by the stimulus program and analyzed using a CCA-based method (Fig. 3), which has been widely used to detect SSVEPs in EEG signals. Given two multidimensional variables \mathbf{X} and \mathbf{Y} and their linear combination $\mathbf{x} = \mathbf{X}^T \mathbf{U}$ and $\mathbf{y} = \mathbf{Y}^T \mathbf{V}$, the CCA attempts to identify the weight vectors \mathbf{U} and \mathbf{V} that maximize the correlation between \mathbf{x} and \mathbf{y} by solving the following optimization problem [39]:

$$\max_{\mathbf{U}, \mathbf{V}} \rho(\mathbf{x}, \mathbf{y}) = \frac{E[\mathbf{U}^T \mathbf{X} \mathbf{Y}^T \mathbf{V}]}{\sqrt{E[\mathbf{U}^T \mathbf{X} \mathbf{X}^T \mathbf{U}] E[\mathbf{V}^T \mathbf{Y} \mathbf{Y}^T \mathbf{V}]}} \quad (2)$$

where the maximum value of ρ with respect to \mathbf{U} and \mathbf{V} is defined as the maximum canonical correlation. For SSVEP detection, $\mathbf{X} \in R^{C \times D}$ denotes a bandpass-filtered EEG data epoch with a size of C samples per channel and D channels, and \mathbf{Y} is the template data epoch for a frequency-phase stimulus with the same sample length as \mathbf{X} . A \mathbf{Y} with a sinusoidal form

$$\mathbf{Y}_f = \begin{bmatrix} \sin(2\pi f t + \phi) \\ \cos(2\pi f t + \phi) \\ \vdots \\ \sin(2\pi N_h f t + \phi) \\ \cos(2\pi N_h f t + \phi) \end{bmatrix} \quad (3)$$

where f is the stimulation frequency, N_h is the number of harmonics (i.e., 3 in this study) and ϕ is the initial phase.

A combined CCA method has recently been reported that considers not only template data but also individual calibration data to improve the SSVEP detection performance [9], [16], [40], [41]. In this study, N subbands of harmonic components (i.e., $N = 3$ in this study) are first extracted from the test EEG data epoch \mathbf{X} using Butterworth infinite impulse response (IIR) bandpass filters that share the same upper-bound frequency (70 Hz) but have different lower-bound frequencies (i.e., for the n th subband component \mathbf{X}_n , the lower-bound frequency is $6 + (n - 1) \times 7$ Hz). By decomposing SSVEPs into these multiple subband components, the FBCCA method efficiently extracts more harmonic components and thereby improves the frequency detection of SSVEPs [42]. Next, three pairs of weight vectors (\mathbf{U} , \mathbf{V}) were obtained by solving Eq. (2): (i) $\mathbf{U}_{\mathbf{X}_n} \mathbf{Y}_{f_k}$

and $V_{X_n Y_{f_k}}$ were calculated using the n th subband component of the test EEG data epoch X_n and the sine-cosine template data epoch Y_{f_k} , where f_k denotes the stimulation frequency of the k th target. (ii) $U_{X_n \hat{X}_{n,k}}$ and $V_{X_n \hat{X}_{n,k}}$ were calculated using X_n and the n th subband component of the individual calibration data associated with the k th target, $\hat{X}_{n,k}$. The individual calibration data \hat{X} and their subband components were obtained through a calibration process (see the *Calibration* section for details). (iii) $U_{\hat{X}_{n,k} Y_{f_k}}$ and $V_{\hat{X}_{n,k} Y_{f_k}}$ were calculated from $\hat{X}_{n,k}$ and Y_{f_k} .

Then, a vector of correlation coefficients was obtained using these three pairs of weight vectors [16], [41], as shown below.

$$\begin{aligned} \mathbf{r}_{n,k} &= \begin{bmatrix} r_{n,k}(1) \\ r_{n,k}(2) \\ r_{n,k}(3) \\ r_{n,k}(4) \end{bmatrix} \\ &= \begin{bmatrix} \rho(X_n^T U_{X_n Y_{f_k}}, Y_{f_k}^T V_{X_n Y_{f_k}}) \\ \rho(X_n^T U_{X_n \hat{X}_{n,k}}, \hat{X}_{n,k}^T V_{X_n \hat{X}_{n,k}}) \\ \rho(X_n^T U_{X_n Y_{f_k}}, \hat{X}_{n,k}^T U_{\hat{X}_{n,k} Y_{f_k}}) \\ \rho(X_n^T U_{\hat{X}_{n,k} Y_{f_k}}, \hat{X}_{n,k}^T U_{\hat{X}_{n,k} Y_{f_k}}) \end{bmatrix} \end{aligned} \quad (4)$$

where $\rho(\mathbf{a}, \mathbf{b})$ denotes the correlation coefficient between \mathbf{a} and \mathbf{b} . Note that both Y_{f_k} and $\hat{X}_{n,k}$ are previously determined data epochs associated with the k th target. Thus, the feature of the n th subband of the test data epoch X_n associated with the k th target was defined in terms of $\mathbf{r}_{n,k}$:

$$p_{n,k} = \sum_{i=1}^4 \text{sign}(\mathbf{r}_{n,k}(i)) \cdot \mathbf{r}_{n,k}(i)^2 \quad (5)$$

where $\text{sign}()$ is used to preserve the discriminating information because negative correlation coefficients might exist between the two signals being compared. Furthermore, a weight coefficient $w(n)$ was applied to each $p_{n,k}$ because the signal-to-noise ratio (SNR) of the SSVEP harmonic components decreases as the evoked frequency increases. The weight coefficients are defined as follows:

$$w(n) = n^{-a} + b, \quad n \in [1 N] \quad (6)$$

where a and b are constants determined using a grid-search method during offline analysis (1 and 0, respectively, in this study). Finally, the classification feature associated with the test data epoch X and the k th target that is to be used for target identification is defined as a weighted square sum of the correlative features $p_{n,k}$ of all subbands [16], [41]:

$$p_k = \sum_{n=1}^N w(n) \cdot p_{n,k}^2 \quad (7)$$

D. EOG Signal Processing

At the end of each round, six segments with a length of 500 ms each (i.e., 125 sampling points) after the onset of highlights were

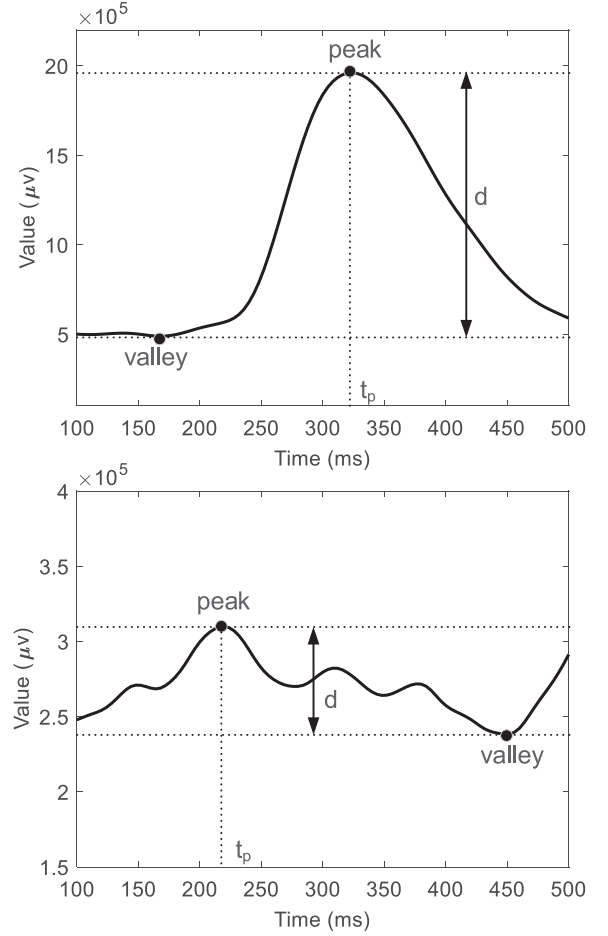


Fig. 4. Comparison of filtered waveforms with and without an eye blink. The x-axis represents the time after the onset of a blinking highlight, d is the distance between the peak and valley values, and t_p is the time delay from the onset of the cue to the peak.

obtained from the recorded EOG signals (Fig. 3), where each EOG segment corresponded to two characters in a group. Next, each segment corresponding to two characters in a group was subjected to baseline drift correction and high-frequency noise removal by applying a bandpass filter at 1–10 Hz [28] to obtain the corresponding EOG feature. These extracted features were then analyzed using the two processes described below.

1) *Waveform detection*: As shown in Fig. 4, an obvious peak occurs in a waveform with a blink, whereas a clear peak is not detected in a nonblink waveform. Here, we use d , which is defined below, to denote the distance between the peak and valley values of the waveform:

$$d = v_{valley} - v_{peak} \quad (8)$$

where v_{valley} and v_{peak} are the minimum and maximum values, respectively, of the EOG segment. Then, a pretrained SVM model for blink detection was used as a regression method to calculate the predicted value y . The model was trained for each subject during his/her EOG calibration (see the *Calibration* section for details). Finally, the following criterion was applied

to each EOG feature vector to detect blinks:

$$r_k = \begin{cases} 1, & \text{if } d > \delta_d \text{ and } y > \delta_y \\ 0, & \text{otherwise} \end{cases} \quad (9)$$

where δ_d and δ_y are two predefined thresholds that vary among subjects. $r_k = 1$ means that the k th segment satisfies the blink detection criterion; otherwise, it does not. Given the parameters d_Θ and y_Θ of the control state (with a blink) and the parameters d_O and y_O of the idle state (without a blink), the thresholds δ_d and δ_y were calculated as follows:

$$\begin{cases} \delta_d = d_O + \alpha_1(d_\Theta - d_O) \\ \delta_y = y_\Theta + \alpha_2(y_\Theta - y_O) \end{cases} \quad (10)$$

where α_1 and α_2 are constant weights determined using a grid-search method (0.8 and 0.6, respectively, in this study).

2) *Candidate Selection*: For a segment that satisfies the blink detection criterion (i.e., $r_k = 1$), an evaluation parameter was then calculated using the following equation:

$$e = |t_p - T_p| \quad (11)$$

where t_p is the time delay from the onset of the cue to the occurrence of the peak in the waveform and T_p is the average delay, which varies across subjects and is determined during the *calibration* process described below. The segments for which the values of the corresponding parameter e ranged from -160 ms to 160 ms were selected as candidates.

E. EEG- and EOG-Based Decision

As shown in Fig. 3, the EEG and EOG data were analyzed independently for SSVEP and blink detection, and the two corresponding candidates were further selected together. In this study, the following three criteria were used to make a decision after these two candidate sets were obtained:

- 1) Criterion I: $[r_1, r_2, \dots, r_m] \cap [s_1, s_2] \neq \emptyset$, where $[r_1, r_2, \dots, r_m]$ are the candidates identified based on blink detection, and $[s_1, s_2]$ are the candidates with top two values for p_k .
- 2) Criterion II: the maximum $p_k >$ the preset threshold δ_1 .
- 3) Criterion III: the ratio of the largest to the second largest value of $p_k >$ the preset threshold δ_2 .

The detailed decision procedure for one trial is depicted in Fig. 5. Once criterion I is satisfied based on the EOG and SSVEP detection results, the system will output the candidate with the largest value of p_k from $[r_1, r_2, \dots, r_m]$ as the target at the end of the current round or next round. Otherwise, no character will be output.

Generally, in the control state, most trials generate the target within one round. However, in a few cases where an eye blink is detected but the user did not sufficiently pay attention to the flickering button to evoke an SSVEP, the correct result for that round might be difficult to obtain due to an inability to satisfy the necessary criteria (i.e., criterion II and criterion III). Therefore, we output the current result until the EEG data from the next round are collected and concatenated with the data from the first round to form an integrated epoch. The user is not required to blink his/her eyes during the second round. Finally, when a character is selected as the result, visual feedback will be

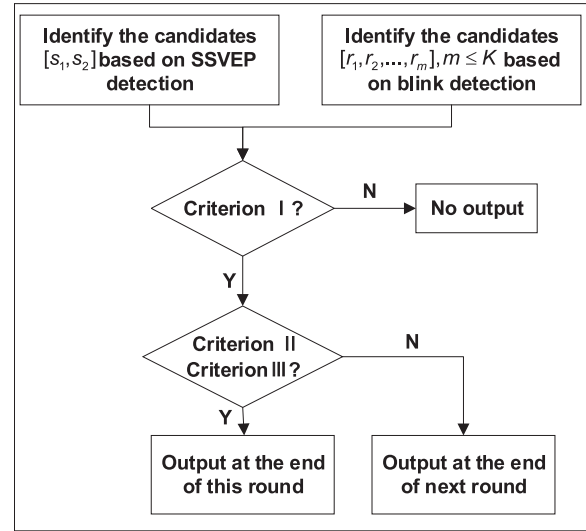


Fig. 5. Schematic of the decision procedure for one trial.

presented for 0.5 s, during which time the text color of the corresponding button turns green and the selected character is typed in the output field.

F. Calibration

Because the EOG and EEG signals vary across subjects, the specific parameters for blink detection (the average delay T_p and the thresholds δ_d and δ_y) and SSVEP detection (the thresholds δ_{p1} and δ_{p2}) were determined individually for each subject. The training datasets for these two signals were collected using the GUI shown in Fig. 2.

The SSVEP training dataset consisted of 48 trials in the control state (4 trials for each character) and 12 trials in the idle state. Prior to each trial, a red visual cue was presented for 0.5 s to indicate a target stimulus, followed by a blank screen for 0.5 s. Each trial lasted for 3 s. During the stimulation period, the subject was asked to fix his/her attention on the target character and avoid eye blinks. In the idle state, the subject was required to avoid highly strenuous events but was allowed to freely blink as usual, close his/her eyes, and perform some basic physiological activities.

Based on the collected EEG data, the epoch length of one detection round for online testing was also set individually for each subject (the results obtained in the current study are presented in Table I). First, a valid range was determined based on the overall offline performance of the subjects. In this study, this range was set to $[1 \text{ s}, 1.6 \text{ s}]$, corresponding to an increasing trend in the average accuracy from 91.46% to 98.33%. The accuracy obtained in the present study was estimated using a leave-one-out paradigm [9]. Then, the epoch length for online test was considered to balance both the accuracy and response time. Basically, we chose the shortest epoch length for each subject as possible with the condition that the corresponding offline accuracy was greater than 92%. Considering the apparent latency of the visual transfer from the eye to the visual

TABLE I
RESULTS OF AN ONLINE SPELLING TEST WITH THE SSVEP- AND EOG-BASED ASYNCHRONOUS SYSTEM

Subject	Epoch length	Mean RT (s)	Accuracy (%)	FPR (%)	ITR (bits/min)
S1	1.0	1.00	95.83	1.00	127.64
S2	1.1	1.12	95.83	0.27	120.16
S3	1.4	1.43	95.83	0.63	99.24
S4	1.4	1.40	95.83	0.63	100.77
S5	1.2	1.30	91.67	1.13	96.10
S6	1.2	1.25	91.67	0.57	98.84
S7	1.4	1.63	97.92	0.00	106.32
S8	1.4	1.43	95.83	2.53	99.20
S9	1.4	1.52	95.83	1.27	94.78
S10	1.3	1.30	97.92	0.00	112.23
Mean \pm SD	1.28 \pm 0.15	1.34 \pm 0.19	95.42 \pm 2.15	0.80 \pm 0.75	105.53 \pm 11.06

cortex [43], a delay τ of 140 ms (see Fig. 3) was selected based on the highest achieved classification accuracy.

Furthermore, as described in the *EEG Signal Processing* section, we extracted the subband features and calculated all final weighted values p_k in both the control state ($p_{k\Theta}$) and the idle state (p_{kO}). Then, we defined the thresholds for online SSVEP detection as follows:

$$\begin{cases} \delta_{p_1} = \beta_1 \cdot (p_{kO})_{mean} \\ \delta_{p_2} = \eta_{min} + \beta_2 \cdot (\eta_{mean} - \eta_{min}) \end{cases} \quad (12)$$

where β_1 and β_2 are constant weights with values in the range of 0 to 1, $(p_{kO})_{mean}$ represents the mean value of p_k in the idle state, and η_{mean} and η_{min} represent the mean and minimum values, respectively, of $\eta = p_{k\Theta}/p_{kO}$.

The EOG training dataset consisted of 10 trials in the control state and 10 trials in the idle state. In the control state, the user was required to blink his/her eyes in synchrony with the cues presented by the system. The requirements for the idle state were the same as in the SSVEP calibration procedure.

The collected EOG signals were used to extract the waveform feature vectors. The average time to reach the maximum value among the 10 blink segments was selected as the average delay T_p . The average distances between the peak and valley values with a blink (d_{Θ}) and without a blink (d_O) were calculated separately. Subsequently, a linear SVM model was trained based on the 10 control state vectors (labeled 1) and 10 idle state vectors (labeled 0) using the LIBSVM toolbox. Hence, the regression values with a blink (y_{Θ}) and without a blink (y_O) were obtained. Then, the EOG thresholds δ_d and δ_y were calculated using Eq. (10).

III. EXPERIMENTS AND RESULTS

We recruited ten healthy subjects with normal vision (all males, 21 to 27 years of age) to participate in the experiments. All subjects provided informed consent for their data to be published. This study was approved by Ethics Committee of Sichuan Provincial Rehabilitation Hospital (approval number: CKLL-2018008), which is our cooperating institution. All subjects were first instructed to perform the calibration data collection

procedure, as described in *Section II-F: Calibration*. Next, two online experiments were conducted, as described below.

A. Experiment I: Free Spelling Test

In this experiment, we first tested the online performance of the participants on a free spelling task in asynchronous mode using the proposed SSVEP- and EOG-based system. All subjects were asked to first select 48 predesignated characters (i.e., each of the 12 characters on the screen were required to be selected four times) in asynchronous mode and then to remain in the idle state for 10 minutes to assess the FPR. When a subject was ready to select a character, he/she was required to gaze at the correct flickering button, blink his/her eyes rapidly after the button was highlighted (size change in this study), and then focus his/her visual attention back on the flickering button. If no character was output at the end of the current round, the subject was required to continue to gaze at the button without blinking in the next round. The start time for the subject to select next target character was determined by himself/herself (self-paced). The procedures are described in more detail in *Section II-E*.

The accuracy, mean response time (abbreviation: RT; unit: s) for selecting a single target, and ITR (unit: bits/min) in the control state and FPR in the idle state were calculated to quantitatively evaluate the online performance of the subjects. Additionally, the mean value and standard deviation (SD) among all subjects were also calculated. The results are shown in *Table I*. The FPR in the idle state [18], [44] was defined using the following equation:

$$FPR = \frac{FP}{TN + FP} \quad (13)$$

where FP and TN were the numbers of false-positive decisions and true-negative decisions in the idle state (10 minutes in this study), respectively. Specifically, the idle period was partitioned into several time intervals, where the length of each time interval was the same as the epoch length of one detection round in the control state. Furthermore, a detection was performed at the end of each time interval, and a TN was counted by the system if there was no character output, otherwise, an FP would be counted. Moreover, the ITR is widely used to evaluate BCI

TABLE II
RESULTS OF AN ONLINE SPELLING TEST WITH THE SSVEP-BASED ASYNCHRONOUS SYSTEM

Subject	Epoch length	Mean RT (s)	Accuracy (%)	FPR (%)	ITR (bits/min)
S1	1.0	1.06	95.83	10.00	119.66
S2	1.1	1.40	95.83	4.80	100.77
S3	1.4	1.53	93.75	15.2	89.60
S4	1.4	1.63	93.75	12.03	85.27
S5	1.2	1.32	97.92	16.43	110.99
S6	1.2	1.60	97.92	24.37	96.19
S7	1.4	1.87	97.92	1.27	85.24
S8	1.4	1.75	97.92	17.73	89.78
S9	1.4	2.22	75.00	24.70	42.16
S10	1.3	1.33	100.00	1.20	117.54
Mean \pm SD	1.28 \pm 0.15	1.57 \pm 0.33	94.58 \pm 7.16	12.77 \pm 8.55	93.72 \pm 22.18

performance [45]:

$$ITR = 60 \left(\log_2 M + P \log_2 P + (1 - P) \log_2 \left(\frac{1 - P}{M - 1} \right) \right) / T \quad (14)$$

where M is the number of characters, P is the accuracy and T is the mean response time for one selection. Note that the trial shifting time (0.5 s) was included in the actual response time when calculating the ITR in this experiment.

On average, satisfactory performance was achieved by all subjects, with a high accuracy (95.42% \pm 2.15%), a relatively high ITR (105.53 bits/min \pm 11.06 bits/min), and a short response time (1.34 s \pm 0.16 s) in the control state and a low FPR (0.80% \pm 0.75%) in the idle state.

Next, a conventional SSVEP-based asynchronous system was designed and tested as a control for comparison with the hybrid asynchronous BCI system. Based on the previous calibration analysis, we first determined the thresholds of the system. Again, 48 free spelling trials were performed, followed by a task of maintaining the idle state for 10 minutes. In addition, the same trial shifting time and epoch length were used as in the hybrid-mode test. Although the self-paced mode was provided, the subjects often chose not to rest for long periods (e.g., for no more than 10 s or even just for the trial shifting time of 0.5 s) before selecting the next character to save time during the free spelling task.

Based on the data collected in each trial, the program decided whether to output a particular character in accordance with the same decision procedure described in Section II-E. The only difference was that all criteria related to EOG data were ignored. During the experiment, if no result was output within five consecutive epochs, the subject was instructed to switch to the next target, and an unsuccessful selection was recorded.

Table II lists the detailed results achieved by the subjects, including the epoch length, response time, accuracy, and ITR in the control state and FPR in the idle state. Using the same trial shifting time of 0.5 s, the average response times ranged from 1.06 to 2.22 s, and an average accuracy of 94.58% \pm 7.16% was achieved, leading to an average ITR of 93.72 bits/min \pm 22.18 bits/min. The minimal and maximal ITRs for all subjects were 42.16 bits/min and 119.66 bits/min, which were achieved

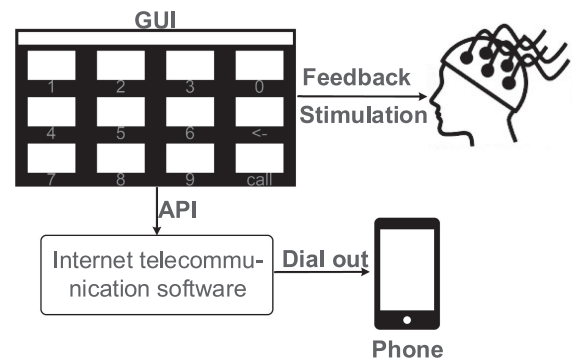


Fig. 6. Diagram of the SSVEP- and EOG-based asynchronous system for phone calls.

by S1 and S9, respectively. However, an average FPR of 12.77% was also recorded.

B. Experiment II: Phone-Dialing Test With the Hybrid Asynchronous BCI System

We developed a simple phone call platform based on the spelling paradigm to further investigate the effectiveness of our hybrid asynchronous system in a practical application, as depicted in Fig. 6. The computer was connected to a mobile phone through the telecommunication software application Skype with the application programming interface (API) provided for developers. The 3 \times 4 stimulus button matrix constituted a virtual telephone keypad, including ten digits (0–9), BACKSPACE (left arrow), and CALL. The user was able to input a set of characters corresponding to a phone number into the text display field, delete an incorrect input by choosing the BACKSPACE button, and dial the number by selecting the CALL button. In this experiment, the subjects were asked to dial their own phone number (eleven-digit numbers) two or three times while taking rests of several seconds when needed. The epoch length of a round for each subject was identical to Experiment I. Finally, the total number of characters required to be input, the entire time required to select characters and rest, the number of incorrect selections, and the number of false positives while resting (where

TABLE III
RESULTS OF THE PHONE NUMBER INPUT TEST

Subject	Numbers dialed	Time (s)	Incorrect selections	False positives
S1	36	140	0	0
S2	36	149	1	0
S3	24	175	3	0
S4	24	90	0	0
S5	24	182	4	1
S6	24	156	5	0
S7	36	211	2	1
S8	24	144	1	0
S9	36	159	4	0
S10	36	202	0	0
Mean \pm SD	30 \pm 6.32	160.8 \pm 34.57	2 \pm 1.89	0.2 \pm 0.42

The characters for one call consist of eleven digits and one dial button.

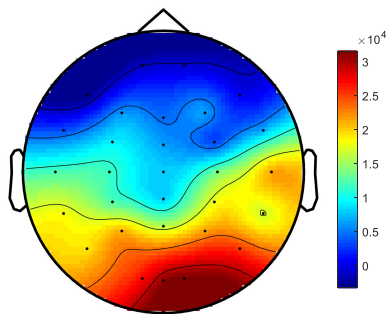


Fig. 7. Group-averaged scalp distribution of 2-s bandpass-filtered SSVEPs. The signals for each channel were filtered to a range of 6–70 Hz with an 11th-order Butterworth bandpass filter and then averaged over all flickering frequencies and all subjects.

the resting duration was not fixed for each subject) were recorded (see Table III).

Generally, all subjects accomplished this task successfully, with almost no false-positive outputs recorded during their resting times (ranging from 10 s to 30 s). The average accuracy calculated during this dialing test was 93.22%, and a significant difference was not observed compared with the accuracy achieved in the hybrid-mode test in Experiment I.

C. EEG Topography and Time-Frequency Analysis

We plotted the topography of the power distribution on the scalp to obtain an intuitive visualization and investigate the physiological plausibility of the SSVEP signals, as shown in Fig. 7. The areas near the occipital and parietal lobes (e.g., CPz, P7, P3, Pz, P4, P8, O1, Oz and O2) displayed the SSVEP signals with the highest energy.

Moreover, Fig. 8 illustrates the impact of eye blink actions on SSVEPs, where a representative example including waveforms (left panel), power spectra (middle panel), and a time-frequency analysis (right panel) of SSVEP signals with and without the blinking task is presented. The eye blink action occurred at 160 ms (indicated with a red dotted line) after the onset of

SSVEP stimulation. The left panel shows that no apparent EOG waveforms similar to the waveforms depicted in the top panel of Fig. 4 were observed under the condition of eye blinking, while the middle and right panels revealed comparable responses at the fundamental frequency (8.5 Hz) under both conditions.

IV. DISCUSSION

In this study, a hybrid asynchronous BCI system combining SSVEP and EOG signals was proposed to enable users to perform self-paced character input. The buttons in the GUI flicker at different fixed frequencies and phases to evoke SSVEPs and are simultaneously highlighted by changing their sizes. SSVEPs are evoked through the JFPM paradigm [16], in which the phase coding is incorporated into the frequency coding, as shown in Eq. (1). Specifically, different initial phases (denoted by $\phi_0 + (k - 1)\Delta\phi$) are manifested in the sinusoidal stimulation by modulating the luminance of these flickering buttons, thereby could be included in the different SSVEP signals. These different initial phases are introduced to enhance the differentiation between frequency-coded targets [9], [16], [18]. Note that we add phase information into the template data of Y_f in this study such that the templates have formal consistence with the stimulus functions. In fact, we can also use the template data of sinusoidal and cosinoidal signals without phase information as in [16]. It could be confirmed that the same results would be obtained by CCA when two sets of different templates of Y_f with the same frequency and different initial phases are used. The user is able to select a character to issue a corresponding command by focusing on its frequency-phase stimulus and simultaneously blinking his/her eyes in accordance with its highlight. The target character is identified through SSVEP and blink detection. Two experiments involving character input and phone dialing were conducted with ten healthy subjects, and the results of the experiment confirm the effectiveness and potential application of the hybrid BCI system (average ITR: 105.52 bits/min; average accuracy: 95.42%; average response time when a command is issued: 1.34 s; and average FPR: 0.8%).

For EEG-based asynchronous BCI systems, the main challenge is to determine appropriate thresholds that quickly and accurately identify a subject's intent to issue a command [18], [23], [25]. Generally, in traditional synchronous scenarios, such as spelling, the character with the highest probability value (e.g., the maximum value of p_k in this study) is chosen as the target class, regardless of the variability among trials. However, in asynchronous applications, the most likely character is an inappropriate output at any period because the starting time for the user's commands has not been determined. Furthermore, the simple preset thresholds are unable to effectively distinguish the control state or idle state due to the intertrial fluctuations in the continuously recorded EEG data. Therefore, additional time-threshold criteria should typically be considered to decrease the FPR in the idle state [18], [46], such as using strict user-dependent thresholds or prolonging the decision time, which may cause fatigue in the subjects.

In this hybrid asynchronous BCI system, discrimination between the control and idle states is mainly achieved through blink

TABLE IV
COMPARISON BETWEEN OUR SYSTEM AND SEVERAL STATE-OF-THE-ART EEG-/EOG-BASED ASYNCHRONOUS SYSTEMS

EEG-/EOG-based asynchronous system	Signal	RT (s)	Number of commands	Accuracy (%)	FPR (%)	ITR (bits/min)
He et al. [27]	EOG	4.14	40	93.02	0.21*	45.83
Panicker et al. [48]	P300+SSVEP	—	36	88.15	4.2	19.05
Zhang et al. [25]	P300	$\geq 2.7^*$	9	—	$\geq 3.79^*$	20 – 27
Zhang et al. [49]	N200	$\geq 9.6^*$	36	92.80	$\geq 6.71^*$	$\leq 26.30^*$
Xia et al. [44]	SSVEP	3	4	77.06	2.37	14.73*
Zhang et al. [18]	SSVEP	≥ 3	3	91.66	$\geq 1.75^*$	≤ 23.8
Townsend et al. [23]	Motor Imagery	4	2	79.33*	30.22*	—
Proposed approach	SSVEP+EOG	1.34	12	95.42	0.80	105.53

— denotes not reported * The value was calculated from the results reported by the authors.

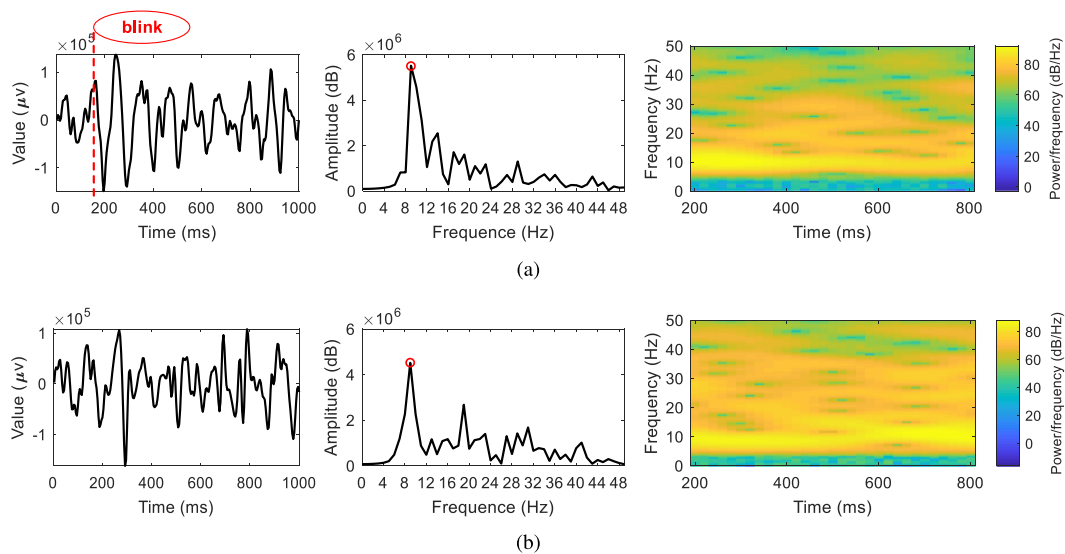


Fig. 8. A representative example including waveforms, power spectra and spectrograms of an SSVEP (1 s of data length) evoked at 8.5 Hz with (a) and without (b) blinking is shown. The amplitude spectra were calculated using a fast Fourier transform, and the red circle indicates the fundamental frequency of 8.5 Hz. The data collected under both conditions were filtered to a range of 6–70 Hz with an 11th-order Butterworth bandpass filter and averaged over all selected 9 channels.

detection because EOG signals are more consistent and easier to detect than EEG signals. Consequently, a relatively lax threshold condition has been used for EEG recognition while maintaining both a low FPR and a short response time. Based on the results of the online spelling tests performed in Experiment I, compared with the conventional SSVEP-based system, our hybrid system achieved a much lower FPR ($0.80 \pm 0.75\%$ vs. $12.77 \pm 8.55\%$ on average, $p = 0.0020$, Wilcoxon signed-rank test) and shorter response time (1.34 ± 0.19 s vs. 1.57 ± 0.33 s on average, $p = 0.0020$, Wilcoxon signed-rank test).

Moreover, the hybrid asynchronous BCI system achieved a high ITR with satisfactory accuracy in the control state using the output strategy that considers both the results of EEG and EOG signal processing. Once the control intention has been detected, approximately 6 EOG candidates among all 12 characters are able to be further selected via EEG signal processing. On the one hand, the use of multiple EOG candidates helps ensure that the target is not generally missed by the user since he/she is not

required to react to the visual highlight extremely quickly and precisely, as in some EOG-only-based spelling systems [27], [47]. In a few cases where blinks occurred too late or too early, the target characters were not selected into the group of candidates for EOG. The characters selected according to EOG data are less likely to be selected as the candidates for SSVEPs because they are not visually attended. Therefore, no character output might occur for the current trial, as we applied the criterion I that the candidates for EOG and top 2 candidates for SSVEP must intersect before the final output is generated. On the other hand, this approach also assists in the process of SSVEP classification by enabling the choice of the final target from among the reduced set of candidates. Comparable accuracy in the control state was achieved for the proposed hybrid asynchronous BCI system, and no significant difference in accuracy was observed between this system and the conventional SSVEP-based asynchronous system ($95.42 \pm 2.15\%$ vs. $94.58 \pm 7.16\%$, $p = 0.7813$, Wilcoxon signed-rank

test). However, a significant difference was observed in the ITR between the proposed system and the conventional system (105.53 ± 11.06 bits/min vs. 93.72 ± 22.18 bits/min, $p = 0.0488$, Wilcoxon signed-rank test). Therefore, we concluded that our system outperformed the SSVEP-based asynchronous system when the RT, ITR and FPR were considered together.

Recently, many EOG or EEG patterns, including P300 potentials, N200 potentials, and SSVEPs, have been widely used to develop asynchronous BCI systems. For example, He *et al.* [27] proposed a single-channel EOG-based speller, whereas Panicker *et al.* [48], Zhang *et al.* [25], Zhang *et al.* [49], Xia *et al.* [44], and Townsend *et al.* [23] reported several different asynchronous BCI systems based on EEG signals. Compared with these systems, the proposed hybrid asynchronous system achieves the highest ITR, the shortest response time, and the highest accuracy. Furthermore, regarding the FPR, another important indicator used to assess an asynchronous system, our method achieves one of the lowest values, second only to the system reported in the study by He and colleagues [27], which achieves its low FPR at the cost of a longer response time (4.14 s) because three rounds of EOG are used for output detection. Finally, in our study, the data were analyzed based on real-time online tests rather than in the simulated online tests described by Zhang and colleagues [18], in which the reported average offline FPR was 11.2%.

Notably, the blinking action will not exert a substantial effect on the SSVEP performance for three reasons. First, the EOG cues are presented by changing the size of the button while maintaining the flicker rate. Second, the eye blink component is concentrated in the forehead (e.g., Fp1 and Fp2), which are located far from the areas (e.g., CPz, P7, P3, Pz, P4, P8, O1, Oz and O2) with the SSVEP signals presenting the greatest energy (Fig. 7). Third, EOG signals appear at low frequencies, while SSVEPs appear in moderate- and high-frequency bands, according to the settings used in this study. This finding was also shown in Fig. 8 indicating that comparable SSVEPs were evoked with or without eye blinking.

Our hybrid system exhibited an acceptable level of comfort for all subjects, although it involved multiple tasks. This comfort level was primarily achieved because the system operated in a self-paced mode, and the subjects were able to rest at any time. Furthermore, the task requiring the subjects to blink their eyes according to the corresponding highlights of buttons is not difficult. Finally, during the idle period, the subjects were able to look at the buttons or screen, which is not allowed in a conventional SSVEP asynchronous mode to avoid false-positive outputs.

V. CONCLUSION

In summary, this study presents a novel hybrid asynchronous BCI system based on SSVEP and EOG signals. Increased discrimination between the control state and the idle state is mainly achieved through blink detection, with SSVEP detection playing an assisting role. Meanwhile, a high accuracy and a short response time are achieved when a command is issued in the control state mainly through SSVEP detection, with blink detection

playing an assisting role. The results of the experiments confirm the satisfactory performance of our hybrid asynchronous BCI system. In a future study, we will introduce transfer learning into our system to simplify or even eliminate the calibration process and will expand the applications of our system to provide assistance for patients with severe paralysis.

REFERENCES

- [1] M. A. Lebedev and M. A. Nicolelis, "Brain-machine interfaces: Past, present and future," *TRENDS Neurosci.*, vol. 29, no. 9, pp. 536–546, 2006.
- [2] N. Birbaumer *et al.*, "Guest editorial brain-computer interface technology: A review of the second international meeting," *Nature*, vol. 398, no. 6725, pp. 297–298, 1999.
- [3] T. Hinterberger *et al.*, "Neuronal mechanisms underlying control of a brain-computer interface," *Eur. J. Neurosci.*, vol. 21, no. 11, pp. 3169–3181, 2005.
- [4] Y. Zhang *et al.*, "Spatial-temporal discriminant analysis for ERP-based brain-computer interface," *IEEE Trans. Neural Syst. Rehabil. Eng.*, vol. 21, no. 2, pp. 233–243, 2013.
- [5] J. Long, Y. Li, and Z. Yu, "A semi-supervised support vector machine approach for parameter setting in motor imagery-based brain computer interfaces," *Cognitive Neurodynamics*, vol. 4, no. 3, pp. 207–216, 2010.
- [6] L. A. Farwell and E. Donchin, "Talking off the top of your head: Toward a mental prosthesis utilizing event-related brain potentials," *Electroencephalogr. Clin. Neurophysiol.*, vol. 70, no. 6, pp. 510–523, 1988.
- [7] G. Townsend and V. Platsko, "Pushing the P300-based brain-computer interface beyond 100 bpm: Extending performance guided constraints into the temporal domain," *J. Neural Eng.*, vol. 13, no. 2, 2016, Art. no. 026024.
- [8] N. V. Manyakov, N. Chumerin, and M. M. Van Hulle, "Multichannel decoding for phase-coded SSVEP brain-computer interface," *Int. J. Neural Syst.*, vol. 22, no. 05, 2012, Art. no. 1250022.
- [9] Y. Zhang *et al.*, "Frequency recognition in SSVEP-based BCI using multitest canonical correlation analysis," *Int. J. Neural Syst.*, vol. 24, no. 4, 2014, Art. no. 1450013.
- [10] P. Yuan *et al.*, "A study of the existing problems of estimating the information transfer rate in online brain-computer interfaces," *J. Neural Eng.*, vol. 10, no. 2, 2013, Art. no. 026014.
- [11] Z. M. Zhang and Z. D. Deng, "A kernel canonical correlation analysis based idle-state detection method for SSVEP-based brain-computer interfaces," in *Proc. Advanced Mater. Res.*, 2012, vol. 341, pp. 634–640.
- [12] F. Galán *et al.*, "A brain-actuated wheelchair: Asynchronous and non-invasive brain-computer interfaces for continuous control of robots," *Clin. Neurophysiol.*, vol. 119, no. 9, pp. 2159–2169, 2008.
- [13] G. R. Müller-Putz *et al.*, "Steady-state visual evoked potential (SSVEP)-based communication: Impact of harmonic frequency components," *J. Neural Eng.*, vol. 2, no. 4, pp. 123–130, 2005.
- [14] M. Cheng *et al.*, "Design and implementation of a brain-computer interface with high transfer rates," *IEEE Trans. Biomed. Eng.*, vol. 49, no. 10, pp. 1181–1186, 2002.
- [15] Z. Lin *et al.*, "Frequency recognition based on canonical correlation analysis for SSVEP-based BCIs," *IEEE Trans. Biomed. Eng.*, vol. 53, no. 12, pp. 2610–2614, 2006.
- [16] X. Chen *et al.*, "High-speed spelling with a noninvasive brain-computer interface," *Proc. Nat. Academy Sci.*, vol. 112, no. 44, pp. E6058–E6067, 2015.
- [17] X. Li and Z. Deng, "Research on the fractal feature extraction based SSVEP idle-state detection," *Int. J. Comput. Commun. Eng.*, vol. 1, no. 4, pp. 331–335, 2012.
- [18] D. Zhang *et al.*, "An idle-state detection algorithm for SSVEP-based brain-computer interfaces using a maximum evoked response spatial filter," *Int. J. Neural Syst.*, vol. 25, no. 7, 2015, Art. no. 1550030.
- [19] J. Pan *et al.*, "Discrimination between control and idle states in asynchronous SSVEP-based brain switches: A pseudo-key-based approach," *IEEE Trans. Neural Syst. Rehabil. Eng.*, vol. 21, no. 3, pp. 435–443, 2013.
- [20] G. Pfurtscheller *et al.*, "Mu rhythm (DE) synchronization and EEG single-trial classification of different motor imagery tasks," *NeuroImage*, vol. 31, no. 1, pp. 153–159, 2006.
- [21] L. He *et al.*, "Channel selection by Rayleigh coefficient maximization based genetic algorithm for classifying single-trial motor imagery EEG," *Neurocomputing*, vol. 121, pp. 423–433, 2013.

- [22] R. Liu *et al.*, "EEG classification with a sequential decision-making method in motor imagery BCI," *Int. J. Neural Syst.*, vol. 27, no. 08, 2017, Art. no. 1750046.
- [23] G. Townsend, B. Graimann, and G. Pfurtscheller, "Continuous EEG classification during motor imagery-simulation of an asynchronous BCI," *IEEE Trans. Neural Syst. Rehabil. Eng.*, vol. 12, no. 2, pp. 258–265, 2004.
- [24] V. Martínez-Cagigal *et al.*, "An asynchronous P300-based brain-computer interface web browser for severely disabled people," *IEEE Trans. Neural Syst. Rehabil. Eng.*, vol. 25, no. 8, pp. 1332–1342, 2017.
- [25] H. Zhang, C. Guan, and C. Wang, "Asynchronous P300-based brain-computer interfaces: A computational approach with statistical models," *IEEE Trans. Biomed. Eng.*, vol. 55, no. 6, pp. 1754–1763, 2008.
- [26] A. Bulling *et al.*, "Eye movement analysis for activity recognition using electrooculography," *IEEE Trans. Pattern Anal. Mach. Intell.*, vol. 33, no. 4, pp. 741–753, 2011.
- [27] S. He and Y. Li, "A single-channel EOG-based speller," *IEEE Trans. Neural Syst. Rehabil. Eng.*, vol. 25, no. 11, pp. 1978–1987, 2017.
- [28] J. Ma *et al.*, "A novel EOG/EEG hybrid human-machine interface adopting eye movements and ERPs: Application to robot control," *IEEE Trans. Biomed. Eng.*, vol. 62, no. 3, pp. 876–889, 2015.
- [29] G. Pfurtscheller *et al.*, "The hybrid BCI," *Frontiers Neurosci.*, vol. 4, pp. 1–11, 2010.
- [30] T. Yu *et al.*, "Enhanced motor imagery training using a hybrid BCI with feedback," *IEEE Trans. Biomed. Eng.*, vol. 62, no. 7, pp. 1706–1717, 2015.
- [31] J.-H. Lim *et al.*, "Development of a hybrid mental spelling system combining SSVEP-based brain-computer interface and webcam-based eye tracking," *Biomed. Signal Process. Control*, vol. 21, pp. 99–104, 2015.
- [32] J. Shin, K.-R. Müller, and H.-J. Hwang, "Eyes-closed hybrid brain-computer interface employing frontal brain activation," *PLoS one*, vol. 13, no. 5, 2018, Art. no. e0196359.
- [33] J. Shin *et al.*, "Improvement of information transfer rates using a hybrid EEG-NIRS brain-computer interface with a short trial length: Offline and pseudo-online analyses," *Sensors*, vol. 18, no. 6, 2018, p. 1827.
- [34] G. Pfurtscheller *et al.*, "Self-paced operation of an SSVEP-based orthosis with and without an imagery-based brain switch: A feasibility study towards a hybrid BCI," *IEEE Trans. Neural Syst. Rehabil. Eng.*, vol. 18, no. 4, pp. 409–414, 2010.
- [35] Y. Li *et al.*, "A hybrid BCI system combining P300 and SSVEP and its application to wheelchair control," *IEEE Trans. Biomed. Eng.*, vol. 60, no. 11, pp. 3156–3166, 2013.
- [36] A. Usakli *et al.*, "A hybrid platform based on EOG and EEG signals to restore communication for patients afflicted with progressive motor neuron diseases," in *Proc. IEEE Eng. Medicine Biol. Soc., Annu. Int. Conf.*, 2009, pp. 543–546.
- [37] H. H. Jasper, "The ten-twenty electrode system of the international federation," *Electroencephalogr. Clin. Neurophysiol.*, vol. 10, pp. 370–375, 1958.
- [38] X. Chen *et al.*, "A high-ITR SSVEP-based BCI speller," *Brain-Comput. Interfaces*, vol. 1, no. 3-4, pp. 181–191, 2014.
- [39] T. W. Anderson, *An Introduction to Multivariate Statistical Analysis*. New York: Wiley, 1962.
- [40] Y. Zhang *et al.*, "SSVEP recognition using common feature analysis in brain-computer interface," *J. Neurosci. Methods*, vol. 244, pp. 8–15, 2015.
- [41] M. Nakanishi *et al.*, "A comparison study of canonical correlation analysis based methods for detecting steady-state visual evoked potentials," *PLoS one*, vol. 10, no. 10, 2015, Art. no. e0140703.
- [42] X. Chen *et al.*, "Filter bank canonical correlation analysis for implementing a high-speed SSVEP-based brain-computer interface," *J. Neural Eng.*, vol. 12, no. 4, 2015, Art. no. 046008.
- [43] D. Regan, "Evoked potentials and evoked magnetic fields in science and medicine," in *Human brain electrophysiology*, 1989, pp. 59–61.
- [44] B. Xia *et al.*, "Asynchronous brain-computer interface based on steady-state visual-evoked potential," *Cognitive Computation*, vol. 5, no. 2, pp. 243–251.
- [45] J. R. Wolpaw *et al.*, "Brain-computer interfaces for communication and control," *Clin. Neurophysiol.*, vol. 113, no. 6, pp. 767–791, 2002.
- [46] P. F. Diez *et al.*, "Asynchronous BCI control using high-frequency SSVEP," *J. Neuroengineering Rehabil.*, vol. 8, no. 1, pp. 1–8, 2011.
- [47] R. Barea *et al.*, "System for assisted mobility using eye movements based on electrooculography," *IEEE Trans. Neural Syst. Rehabil. Eng.*, vol. 10, no. 4, pp. 209–218, 2002.
- [48] R. C. Panicker, S. Puthusserypady, and Y. Sun, "An asynchronous P300 BCI with SSVEP-based control state detection," *IEEE Trans. Biomed. Eng.*, vol. 58, no. 6, pp. 1781–1788, 2011.
- [49] D. Zhang *et al.*, "An N200 speller integrating the spatial profile for the detection of the non-control state," *J. Neural Eng.*, vol. 9, no. 2, 2012, Art. no. 026016.